Highly ordered monocrystalline silver nanowire arrays

G. Sauer, G. Brehm, and S. Schneider
*Institute of Physical and Theoretical Chemistry, University Erlangen-Nuremberg, Egerlandstrasse 3,
D-91058 Erlangen, Germany*

K. Nielsch, R. B. Wehrspohn,[a] J. Choi, H. Hofmeister, and U. Gösele
Max-Planck-Institute of Microstructure Physics, Weinberg 2, D-06120 Halle, Germany

Highly ordered silver nanowire arrays have been obtained by pulsed electrodeposition in self-ordered porous alumina templates. Homogeneous filling of all the pores of the alumina template is achieved. The interwire distance is about 110 nm corresponding to a density of silver nanowires of 61×10^9 in.$^{-2}$ and the diameter can be varied between 30 and 70 nm. The silver wires are monocrystalline with some twin lamella defects and grow perpendicular to the $\langle 110 \rangle$ direction. The previously encountered difficulty to obtain 100% filling of the alumina pores is discussed in the framework of electrostatic instabilities taking into account the different potential contributions during electrodeposition. To obtain homogeneously filled pore membranes, a highly conductive metal containing electrolyte, a homogeneous aluminum oxide barrier layer, and pulsed electrodeposition are a prerequisite. © *2002 American Institute of Physics.*
[DOI: 10.1063/1.1435830]

I. INTRODUCTION

We report on the preparation of ordered silver nanowire arrays obtained by pulsed electrodeposition in porous alumina. Nearly 100% filling of the nanometer sized pores with silver has been obtained. The difficulty of achieving a homogeneous filling is based on instabilities occurring during growth of the highly conducting silver nanowires. In other publications concerning filling of nanopores with silver the problem of the homogeneity of the filling is not addressed and it can be deduced from the data that only a very low filling fraction has been achieved.[1–3] Furthermore, so far most people dealing with the filling of porous materials used disordered alumina, track-etched polycarbonate-membranes, or other disordered pore arrays as templates,[4–6] which even in case of homogeneous pore filling would yield disordered wire arrays with a large dispersion in the pore diameter. Possible applications for such ordered wire arrangement include photonic crystals[7] and surface enhanced Raman spectroscopy (SERS).[8] Other applications might be based on the sharp size distribution of the wire dimensions replicating the high order of the template. After dissolving the alumina matrix, these wires can be either used as conducting nanowires in nanodevices or as templates for hollow cylinders similar to hollow spheres.[9] This article is organized as follows. We first report on the porous alumina template preparation. Then we will present the filling procedure and characterize the silver nanowire arrays. Finally we discuss the instabilities occurring during silver nanowire growth in the framework of a linear stability analysis.

[a]Author to whom correspondence should be addressed; electronic mail: wehrspoh@mpi-halle.de

II. TEMPLATE PREPARATION

Hexagonally ordered porous alumina templates have been prepared via a two-step anodization process, which is reported in detail elsewhere.[10–12] Briefly, a first long-duration oxidation of high purity aluminum and subsequent complete dissolution of the formed porous alumina leads to patterned aluminum substrates. The surface keeps the regular hexagonal texture, formed during the first oxidation process by self-assembly, which acts as a mask for the second anodization (Fig. 1). After the second oxidation, an ordered nanopore array is obtained. The diameter and depth of the pores as well as the distance between them and the degree of ordering depends critically on the anodization parameters. Typical parameters used in this work are 0.3 M oxalic acid, $U_{ox} = 40$ V, and $T = 2\,°C$. To obtain homogeneous electrodeposition into the pores in the final step it is highly necessary to previously reduce the alumina barrier thickness at the pore bottom. The thinning is achieved by chemical etching and/or by current limited anodization steps.[13] First, isotropic chemical pore widening reduces the barrier thickness and increases the pore diameter. Then, the sample is oxidized several times for 10–15 min using constant current conditions, reducing the current after each step by a factor of 2. The anodization potential decreases slowly with decreasing barrier thickness. The thinning is stopped when the anodization potential reaches a value of 6 to 7 V, which is equivalent to a barrier layer thickness of about 10 nm. Further thinning might cause the oxide structure to peel off of the aluminum substrate during the deposition. Applying current limited anodization steps not only results in a thinning of the barrier oxide, but also in a modification of the pore structure. The originally straight pores branch out at the formation front because the pore density is inversely proportional to the square of the anodizing potential (Fig. 1).[14,15] The splitting up of the pores
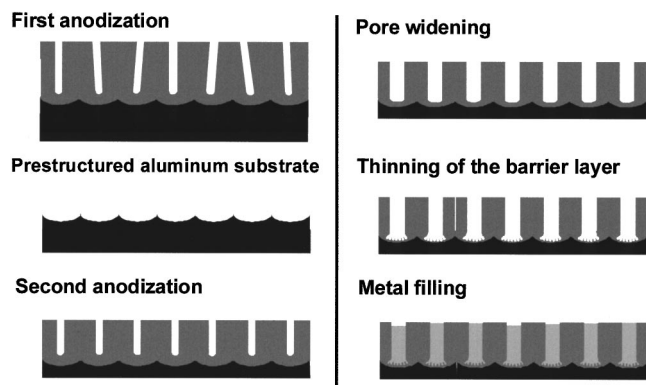
FIG. 1. Schematic diagram describing the fabrication of a highly ordered porous alumina matrix and the preparative steps necessary for the subsequent filling of the structure. The Al substrate is prestructured by a long-time anodizing until the pores arrange in a hexagonal lattice. Then the aluminum oxide is selectively removed. Starting from a prestructured Al substrate, a highly ordered alumina pore structure is obtained in a second anodization step. Afterwards, the barrier layer is thinned and the pores are widened by isotropic chemical etching. For further thinning of the barrier layer two current-limited anodization steps are used and dendrite pore formation occurred at the barrier layer. Then, the pores are filled by pulsed electrodeposition with silver.

FIG. 2. Current and potential transients during electrodeposition. First a current-limited negative pulse t_{pulse} is applied to deposit Ag. Then a positive pulse is applied to discharge the capacitance of the alumina barrier layer. The cycle is repeated after t_{off} in order to avoid depletion of metal ions near the deposition interface.

into the barrier layer leads to the formation of several nucleation sites in each pore at the beginning of the electrodeposition. Since the potential drop at the deposition interface depends critically on the barrier thickness, it has to be highly uniform. This is achieved by our thinning process described above.

III. ELECTRODEPOSITION

The pores are filled with silver under constant current conditions adopting the concept of pulsed electrodeposition. To achieve homogeneous filling of the pores, the choice of a suitable electrolyte is crucial. In order to avoid corrosive attack of the alumina template, the *p*H of the electrolyte has to be adjusted between 4 and 8.[16] Therefore it is hardly possible to work with cyanide containing silver baths, which generally require a higher *p*H. To supply the deposition interface sufficiently fast with metal ions the concentration of electroactive silver species has to be as high as possible, otherwise hydrogen evolution can become dominant. Furthermore, pulsed electrodeposition through an insulating barrier layer requires high negative polarization (U_{pulse} as high as -8 V). Consequently, the electrolyte must not contain other electroactive species like, e.g., nitrate ions, which also might react in side reactions under these conditions. Finally, stability analysis shows (see below) that the conductivity in the electrolyte has to be quite high to obtain uniform deposition into the pores. Based on these considerations the choice of a suitable electrolyte is not trivial. As the presence of nitrate ions and other electroactive species is excluded silver sulfate (8.5 g/l) was chosen as the silver ion source. Diammoniumhydrogencitrate (200 g/l) was added to ensure a high conductivity and to adjust the *p*H value to around 4.5. Furthermore, diammoniumhydrogencitrate has the function of a repairing agent as it favors the formation of stable alumina during the positive polarization in the pulse sequence
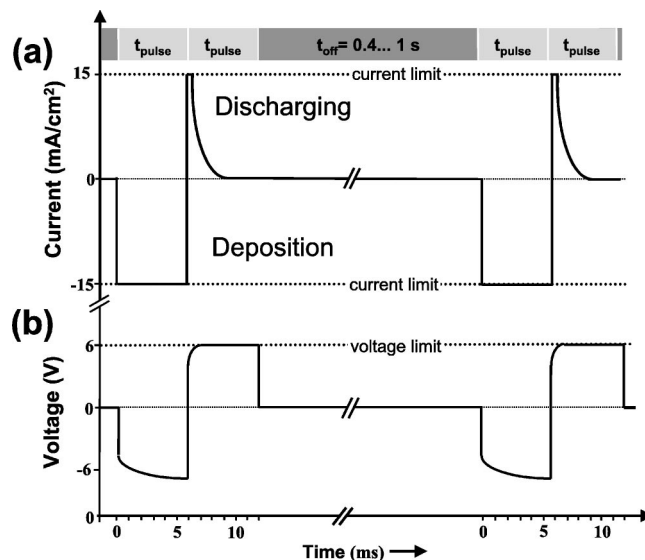
(see below). Finally, the electrolyte contained potassiumthiocyanate (105 g/l), which was necessary to dissolve precipitated silver salt through complexation. The pulsed electrodeposition consists of modulated pulses in the millisecond range (Fig. 2). During each pulse of negative current (t_{pulse} = 6 ms, I_{pulse} = 15 mA/cm^2), silver is deposited at the pore bottom. A relatively high current density is applied in order to increase the number of nucleation sites in each pore.[12] After the deposition pulse, another pulse with positive polarization (t_{pulse} = 6 ms, U_{pulse} = 6 V) was applied to discharge the capacitance of the barrier layer and to interrupt the electric field at the deposition interface immediately. The positive pulse also repairs discontinuities in the barrier oxide, an important mechanism especially at the beginning of the electrodeposition. The current for this second pulse is also limited to I_{max} = 15 mA/cm^2. To avoid depletion of the silver ions at the deposition interface, the ion concentration has to recover before the next double pulse is applied. Introducing a delay time t_{off} of typically 0.4–1 s is sufficient to ensure the restoration of a high silver concentration at the pore bottom before the subsequent deposition pulse appears. This improves the homogeneity of the deposition and prevents excessive hydrogen evolution. During the electrodeposition, the potential required to ensure the desired current density is measured for each pulse. Hence the electrodeposition can easily be followed via a potential versus pulse number plot (Fig. 3). Generally, the plot can be divided into three regions. At the beginning of the filling process the electrons have to tunnel through the barrier oxide before they react with the silver ions and nucleation takes place at numerous sites in each pore. The surface available for electrodeposition is quite large. Further electrodeposition leads to a filling of the branched structure and thus the electrochemically active surface area decreases, accompanied by an increase in the deposition potential (first region). When the deposited silver
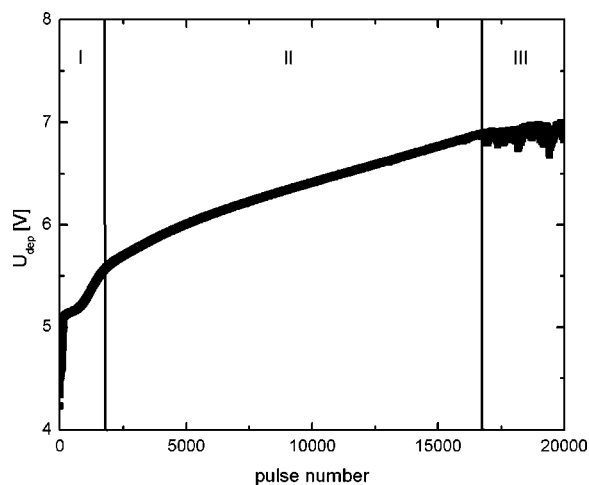
FIG. 3. Voltage-pulse-number curve during the filling process of porous alumina with Ag. In regime I the dendride-like nucleation pores are filled with Ag. The potential increases due to a reduction of the deposition area. In regime II the silver wires grow and the potential increases slightly. In regime III the silver wires reach the top of the alumina template and the noise and slight potential drop are due to the uncontrolled increase in deposition area.

reaches the beginning of the straight part of the pores the increase in the deposition potential slows down distinctly, but still proceeds (second region). The decreasing silver concentration in the pore channel can be made responsible for a gentle increase in the deposition potential in this region, but it cannot explain the significant rise of more than one volt. The filling of the pores continues until the deposition potential drops or exhibits some noise (third region), which is due to an increase of the electroactive surface arising from silver deposition on top of the porous alumina matrix. Although the significant increase in the deposition potential, especially in the second region, is not completely understood yet, the potential versus pulse number plot at least allows one to follow and control the filling process. Additionally the charge can be calculated from the measured data and thus allows one to estimate the degree of pore filling and to control the wire length.

IV. CHARACTERIZATION

The filled alumina templates were examined by scanning electron microscopy (SEM) to determine the degree of pore filling and the extension of the silver nanowires. By etching the filled porous structure from the top, nanowires ending somewhat below the membrane surface became observable for scanning electron microscopy (SEM) examination. Etching of the samples was performed by Ar sputtering with an ion mill (Gatan Duo Mill 600) and led to a funnel-shaped excavation in the surface. The depth of the hole was correlated with the etching time. Figure 4 shows two top view micrographs and one side view micrograph of a highly ordered alumina pore structure filled with silver. The pore diameter is approximately 35 nm and the interpore distance is 110 nm. The thickness of the porous layer is approximately 2 μm. Figure 4(a) was taken before etching the sample. In some pores, the silver nanowires reached the pore opening and excessive electrodeposition yielded three-dimensional growth of silver particles on top of the matrix structure (bright spots). In most of the remaining (not completely filled) pores, the top of the nanowires can be seen (different gray levels indicate different levels of residual pore depth). Figure 4(b) shows the same sample after etching the initially 2 μm thick porous structure by about 200 nm. As can be seen clearly, almost every pore is filled with silver to this level indicating fluctuations in the height of the filling of less than 10%. The same information can be obtained from Fig. 4(c). Simple cutting of an (unthinned) substrate with wire cutting pliers leads to a fracture of the rigid alumina layer. Most of the pores are filled with silver wires (bright sticks) to at least 90% in height. The lack of wires in some of the pores as well as the presence of twisted and ruptured wires can easily be explained by the mechanical stress evolving during the process of the cleavage of the alumina membrane.

Crystallinity and surface configuration of the silver wires were further analyzed by high-resolution transmission electron microscopy (HRTEM). After dissolving the alumina matrix such wires have been placed on electron microscopy copper grids covered by a thin carbon film. Although arranged randomly on the carbon film, the silver wires tend to
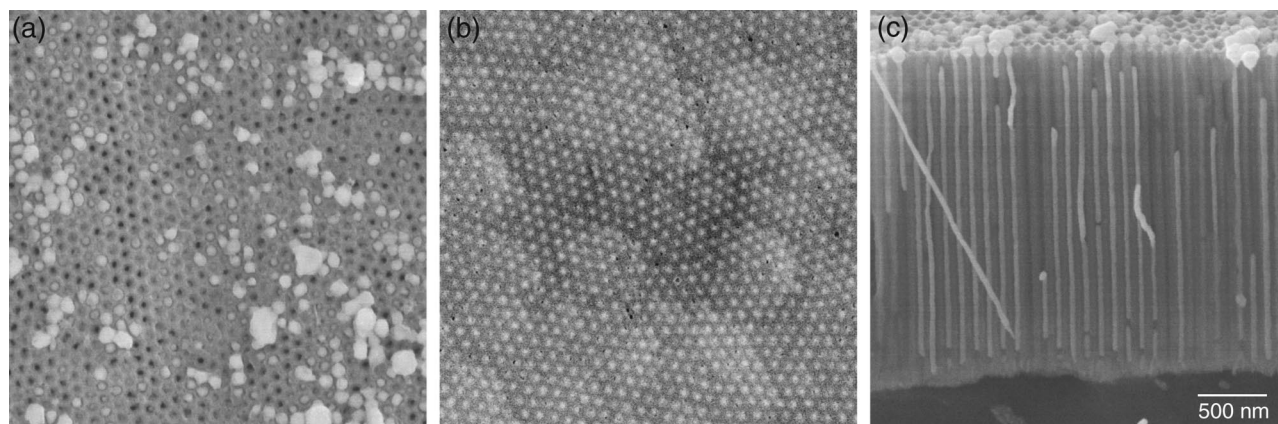

FIG. 4. SEM micrographs of a silver-filled alumina membrane. (a) Top view of an unthinned sample, (b) top view of the same sample approximately 200 nm underneath the initial surface, and (c) side view of a fracture.
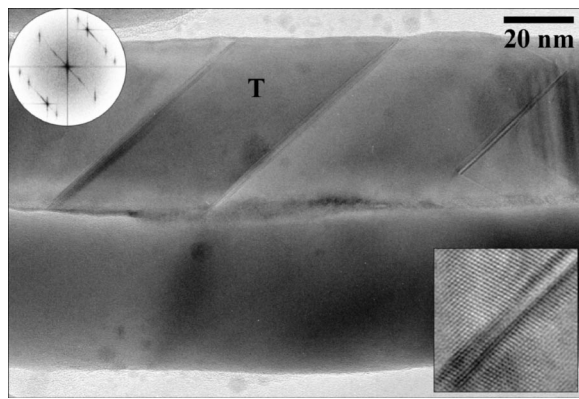
FIG. 5. HRTEM image of a segment of two adjacent silver nanowires. The upper one exhibits three planar defects shown in more detail in the box below. The diffractogram (circular inset) reflects the lattice relation between the twin lamella "T" and wire matrix.

align parallel in groups because of capillary forces acting during evaporation of the solvent. Figure 5 shows a HRTEM image of a segment of two adjacent wires touching each other along a nearly horizontal line. From selected area electron diffraction these silver wires are found to be single crystalline. Nevertheless, they contain a certain extent of lattice defects such as twin boundaries and stacking faults. While the wire in the lower part of Fig. 5 does not exhibit lattice defects in the frame of this image, the upper wire has three planar defects that may be recognized as narrow bands of stronger contrast running obliquely across the wire. Their structures are shown in more detail in the boxes beneath. From the course of the lattice plane fringes seen here, and reflected also by the diffractogram (Fourier transform) of the image given in the circular inset, the $\langle 110 \rangle$ zone axis of the silver lattice is deduced to be perpendicular to the wire axis. The wires have generally a face-centered-cubic (fcc) lattice, which was also confirmed by x-ray diffraction analysis. They do not show indications of neither oxide coverage nor incorporation.
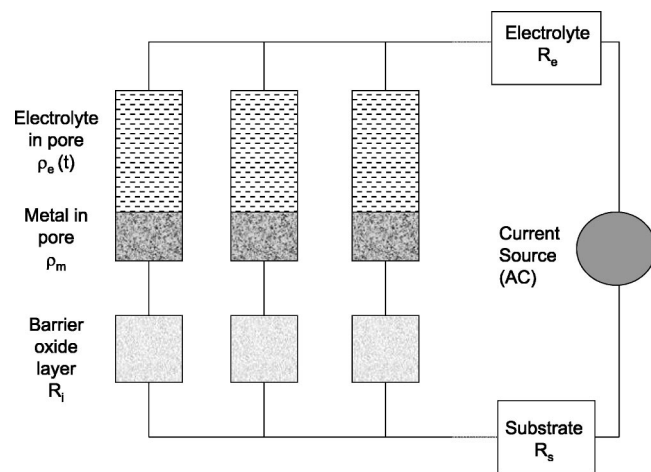

FIG. 6. Schematic diagram of the electric circuit during pulsed electrodeposition.

TABLE I. Resistivities (at 38 °C) of some metals and electrolytes used in this work and similar work in literature.

Material	Resistivity in Ω cm
nickel (bulk)	6.3×10^{-6}
silver (bulk)	1.4×10^{-6}
nickel Watts-bath electrolyte	14
Metzger Co bath	77
Xu Ni bath	500
silver containing electrolyte (this work)	5.2

V. DISCUSSION

As mentioned in the Introduction, most studies have not discussed the achieved degree of filling of the pores with either silver[1–3] or other metals like Au,[17] Co,[18–21] Fe,[22] or Ni.[23] In the present work we demonstrated that under very specific conditions of pulsed electrodeposition, one can obtain a nearly 100% homogeneous filling of pore arrays also with silver. In a former publication we have shown that it is indeed possible to fill homogeneous nickel and cobalt into porous alumina.[13]

Now we are presenting a model to explain the physical reasons underlying this process. The key ingredients of our model are a thin homogeneous barrier layer, pulsed electrodeposition, and a highly conducting electrolyte. Figure 6 shows a schematic diagram of the equivalent electrical circuit applicable during pulsed electrodeposition. Starting from the current source, there is a resistance in the aluminum substrate (R_s), then all the pores are in parallel consisting of a thin interfacial oxide layer (R_i), the deposited metal (ρ_m), and the electrolyte (ρ_e). Finally, there is a common resistance of the electrolyte in the electrochemical cell (R_e). For a stability analysis, we can neglect the potential drop in the aluminum substrate and the electrolyte since they are simple series resistances and do not contribute significantly to the instability. The first instability arises from the fact that the alumina barrier layer at the pore bottom is not uniform. If it would be uniform, then it would represent an overall series resistance like R_e or R_s. However, due to the electrochemical process, there are always fluctuations in the barrier layer thickness. Therefore as already pointed out by Zagiel *et al.*,[24] the barrier layer thickness and therefore the overall potential drop iR_i should be as small as possible compared to the potential drop across ρ_e and ρ_m. This is the reason for thinning the alumina barrier layer to typically 10 nm. However, this still results in a significant contribution to the potential drop of ~ 6 V in the barrier layer compared to a few tenths mV for the electrolyte solution (Table I). Therefore and because of the rectifying nature of the barrier layer, we have applied a self-limiting current process by using pulsed electrodeposition. During the 6 ms negative pulses, all of the metal ions in the pore are deposited due to the high current. Thus once all the ions have been deposited in one specific pore, the current flow is reduced and other pores with a slightly thicker barrier layer take over the current. A uniform filling of the pore bottom is achieved and the impact of fluctuations of R_i is reduced due to a time dependent electrolyte resistivity $\rho_e(t)$. During the positive pulse, the capacitance of

the barrier layer is discharged. Moreover, as pointed out by Dobrev *et al.*,[25] the use of positive pulses leads to monocrystalline nanowires. They speculate that during the positive pulse, a certain amount of current will lead to the preferential dissolution of the defect rich metal deposit of the previous negative pulse, thus promoting monocrystalline growth.

Another electrostatic instability arises during the growth of the silver wires. Since the Ag nanowires are always more conductive than the electrolyte, small fluctuations in the length of the wire will be enhanced and will lead to nonuniform growth. Similar to the case of pore growth in highly resistive *p*-type silicon, this effect can be described by a linear stability model. Following Wehrspohn *et al.*,[26,27] we can define a instability coefficient α

$$\alpha = \frac{\rho_e - \rho_m}{\rho_e + qR_i + \rho_m} q, \tag{1}$$

where q is the fluctuation wavenumber (in cm^{-1}). If α is negative, the metal wire front grows uniformly, i.e., the filling is homogeneous. If α is positive, the metal wire front will in general be unstable and an inhomogeneous filling will occur. The inverse $1/\alpha$ represents the typical length for which one silver wire will start to grow faster in one pore than in the others. To obtain a homogeneous filling because of negative α, the resistivity of the electrolyte must be lower than that of the metal wire. Such a condition is unrealistic for any metal since the conductivity of pure metals ($\sim \mu\Omega\,\text{cm}$) is a few orders of magnitude higher than that of concentrated electrolytes ($\sim 10\ \Omega\,\text{cm}$). The only possibility to fill a thin layer of porous alumina rather homogeneously is therefore to increase $1/\alpha$ so that it is larger than the membrane thickness. This means the onset of the instability will not occur below this critical thickness and a homogeneous filling is possible. Since $\rho_m \ll \rho_e$, the critical thickness $1/\alpha$ simplifies to $1/\alpha = 1/q + R_i/\rho_e$. For $q \approx 10^5\ \text{cm}^{-1}$, $R_i \approx 36\ \Omega\,\text{cm}^2$ for a current density $I = 15\ \text{mA/cm}^2$ and a porosity of 9%, $\rho_e \approx 10\ \Omega\,\text{cm}$, $1/\alpha$ is limited by the term R_i/ρ_e, i.e., interface or barrier-layer limited. Thus the barrier layer thickness is proportional to the critical thickness $1/\alpha$ and the conductivity of the electrolyte is inversely proportional to $1/\alpha$. This underlines the importance of using highly conductive electrolytes like Watts-bath-type electrolytes in the case of Ni and Co nanowires. Indeed, the Xu group[28] and the Metzger group[29] both obtain very good Ni filling degrees in alumina pore arrays applying these rules. Xu uses barrier layer thinning, pulsed electrodeposition, and high temperature deposition to increase the mobility of the ions in the organic electrolyte.[28] Metzger uses pulsed electrodeposition, barrier layer thinning, and also highly conducting electrolytes. However, in both studies, the resistivities are much higher than for the Watts-bath type electrolyte used in our work.[13] Therefore instabilities have to be compensated in these groups by decreased pulse duration. However, a drawback of the latter strategy is that a thicker barrier layer has to be used to reduce the discharge time of the barrier layer capacitance. The thicker barrier layer leads to significantly higher overpotentials during deposition and to a worse crystallinity of the nanowires.[29]

VI. CONCLUSIONS

A highly efficient method of depositing silver into the nanochannels of ordered porous alumina is presented. Nearly 100% of the pores were filled with silver and only small fluctuations in the growth rate in different pores were observed. The silver nanowires are monocrystalline with some twin-lamella defects. The growth direction is perpendicular to the $\langle 110 \rangle$ direction. The wire diameter can be varied from 30 to 70 nm depending on how the alumina template is prepared. Based on a linear stability analysis, we have modeled the electrochemical filling behavior. To obtain homogeneously filled pore membranes, a homogeneous aluminum oxide barrier layer, pulsed electrodeposition, and a highly conductive electrolyte are a prerequisite.

[1] Q. Zhang, Y. Li, D. Xu, and Z. Gu, J. Mater. Sci. Lett. **20**, 925 (2001).
[2] I. Mikuslkas *et al.*, Opt. Mater. **17**, 343 (2001).
[3] F. Müller, A. D. Müller, M. Kröll, and G. Schmid, Appl. Surf. Sci. **171**, 125 (2001).
[4] X. Jiang *et al.*, J. Mater. Chem. **11**, 1775 (2001).
[5] V. M. Cepak and C. R. Martin, J. Phys. Chem. B **102**, 9985 (1998).
[6] N. F. Jana *et al.*, Chem. Commun. (Cambridge) **7**, 617 (2001).
[7] H. van der Lem and A. Moroz, J. Opt. **2**, 395 (2000).
[8] G. Sauer (unpublished).
[9] F. Caruso, R. A. Caruso, and H. Möhwald, Chem. Mater. **11**, 3309 (1999).
[10] H. Masuda and K. Fukuda, Science **268**, 1466 (1995).
[11] H. Masuda, K. Yada, and A. Osaka, Jpn. J. Appl. Phys., Part 2 **37**, L1340 (1998).
[12] O. Jessensky, F. Müller, and U. Gösele, Appl. Phys. Lett. **72**, 1173 (1998).
[13] K. Nielsch, F. Müller, A.-P. Li, and U. Gösele, Adv. Mater. **12**, 582 (2000).
[14] F. Keller, M. S. Hunter, and D. L. Robinson, J. Electrochem. Soc. **100**, 411 (1953).
[15] A.-P. Li, F. Müller, A. Birner, K. Nielsch, and U. Gösele, J. Appl. Phys. **84**, 6023 (1998).
[16] P. P. Mardilovich, A. N. Govyadinov, N. I. Mazurenko, and R. Paterson, J. Membr. Sci. **98**, 143 (1995).
[17] X. Y. Zhang *et al.*, J. Mater. Chem. **11**, 1732 (2001).
[18] H. Zeng, M. Zheng, R. Skomski, D. J. Sellmyer, Y. Liu, L. Menon, and S. Bandyopadhyay, J. Appl. Phys. **87**, 4718 (2000).
[19] A. Kazadi Mukenga Bantu *et al.*, J. Appl. Phys. **89**, 3393 (2001).
[20] T. Thurn-Albrecht, J. Schotter, G. A. Kästle, N. Emley, T. Shibauchi, L. Krusin-Elbaum, K. Guarini, C. T. Black, M. T. Tuominen, and T. P. Russell, Science **290**, 2126 (2000).
[21] H. Q. Cao, Z. Xu, H. Sang, D. Sheng, and C. Y. Tie, Adv. Mater. **13**, 121 (2001).
[22] Y. Peng, H.-L. Zhang, S.-L. Pan, and H.-L. Li, J. Appl. Phys. **87**, 7405 (2000).
[23] P. M. Paulus, F. Luis, M. Kröll, G. Schmid, and L. J. de Jongh, J. Magn. Magn. Mater. **224**, 180 (2001).
[24] A. Zagiel, P. Natishan, and E. Gileadi, Electrochim. Acta **35**, 1019 (1990).
[25] D. Dobrev, J. Vetter, N. Angert, and R. Neumann, Appl. Phys. A: Mater. Sci. Process. **69**, 233 (1999).
[26] R. B. Wehrspohn, J.-N. Chazalviel, and F. Ozanam, J. Electrochem. Soc. **145**, 2958 (1998).
[27] R. B. Wehrspohn, F. Ozanam, and J.-N. Chazalviel, J. Electrochem. Soc. **146**, 3309 (1999).
[28] A. J. Yin, J. Li, W. Jian, A. J. Bennett, and J. M. Xu, Appl. Phys. Lett. **79**, 1039 (2001).
[29] M. Sun, G. Zangari, M. Shamsuzzoha, and R. M. Metzger, Appl. Phys. Lett. **78**, 2964 (2001).